Design and Implementation of A Convex-Optimized Positioning System on Wireless RF/FPGA Platform

Li-Hong Huang, Kai-Ting Shr, Ming-Hung Lin, Yuan-Hao Huang
Institute of Communications Engineering and Department of Electrical Engineering
National Tsing Hua University, Taiwan, R.O.C. 30013
Email: yhhuang@ee.nthu.edu.tw

***Abstract*—This paper presents the design and implementation of a positioning system based on particle filters and a convex optimization processor. The positioning system uses a virtual base-station transform (VBST) and convex optimization algorithm to deal with the none-light-of-sight (NLOS) problem in wireless communication systems. This study designs a modified resampling particle filter to reduce the processing latency with little performance loss. The proposed system uses four modified particle filters to adopt RSS signals from at most four base stations to estimate their distances to the mobile station. Then, the estimated distances are delivered to a convex optimization processor with the VBST algorithm to locate the mobile station. This work implemented the positioning algorithm on Xilinx Virtex-4 FPGA and RF modules to verify the positioning performance. The measurement and analysis results show that the proposed convex-optimized positioning system reduces 20% RMSE in the mixed NLOS/LOS environment compared to the sole particle filtering approach.**

I. Introduction

Location information has been widely used in many applications such as navigation, resource allocation, and healthcare systems [1]–[4]. The most popular global positioning system (GPS) faces performance degradation in urban areas and NLOS environments [5]. Thus, network-based positioning is usually adopted to increase the positioning accuracy. The positioning system often uses received signal strength (RSS) as a metric to map the propagation loss between MS and BS into distance information. A generic RSS-based positioning method may cause 30-40 dB signal gain variation, causing large positioning error. Thus, filtering process, such as Kalman filter [6], is usually adopted to improve the positioning accuracy, but linear Kalman filter cannot handle some non-linear effects in the channel. Thus, a particle filter [7], a recursive Bayesian tracking filter, was proposed to deal with this non-linear problem. None-light-of-the-sight (NLOS) is a big problem that degrades the positioning performance. Research in [8] deals with this problem by building accurate channel model to improve the performance, but this model is usually not available in the practical system. Fingerprinting method can also address the NLOS problem efficiently but it requires high-cost fingerprint database maintenance. The research in [9] proposed to weight the NLOS and LOS contributions in the convex optimization process. Based on this concept, our previous study [10] presents a virtual base-station transform technique and a Manhattan/Euclidean mixed norm as a mapping factor of weight. The database of map factors is much smaller than that of fingerprinting because the map factors are only stored at the crossroads. This paper presents the design and implementation of the mobile positioning system based on latency-reduced particle filters and convex optimization processor for the positioning systems, which were integrated in FPGA and RF TX/RX modules to verify the performance in the mixed NLOS/LOS environment.

The rest of this paper is organized as follows. Section II describes the channel model and positioning algorithm. Section III presents the proposed particle filter and convex optimization processor. Section IV demonstrates the proposed positioning system and the analysis results. Finally, Section V concludes this paper.

II. Positioning System and Algorithms

A. System Model

This study uses the path-loss and log-normal shadowing channel model as follows:

$$P_{rx(dB)} = P_{tx(dB)} + K - 10\alpha \log_{10} d + n_{shadowing}, \quad (1)$$

where $P_{rx(dB)}$ is the RSS in dB, $P_{tx(dB)}$ is the transmitted power, d is the propagation distance, K is the factor of the antenna height and antenna gain, $n_{shadowing}$ is equal to $h^2_{shadowing}$ which represents the log-normal shadowing effect, and α is the path-loss decay ratio. $n_{shadowing}$ is Gaussian distributed in the logarithmic domain. This study further considers the baseband processing aspect as follows:

$$y = hx + n, \quad (2)$$

where h is the channel gain and n is additive white Gaussian noise. Because the channel effect includes the path loss and the log-normal shadowing, this study separates h into three parts: path-loss, shadowing, and fast fading. Then, (2) is equivalent to

$$y = h_{pathloss} h_{shadowing} h_{fast} x + n, \quad (3)$$

where $h_{pathloss}$ equals $sqrt(Kd^{-\alpha})$, $h_{shadowing}$ is log-normal shadowing in signal domain, and h_{fast} is fast fading.

With the reference signal x, the receiver can extract the decay level the from faded signal y. Based on (3), a single received signal y cannot be used to estimate the distance because of h_{fast} and n. Because the shadowing effect is caused by stationary obstructed objects like buildings, we assume that the shadowing effect remains the same within a short time. Hence, we can eliminate h_{fast} and AWGN by averaging the received signals.

TABLE I. SYSTEMATIC RESAMPLING ALGORITHM.

$[\{\mathbf{x}_t^j, w_t^j\}_{i=1}^{N_s}] = \text{RESAMPLE}[\{\mathbf{x}_t^i, w_t^i\}_{i=1}^{N_s}]$
1. Initial the CDF: $c_1 = 0$
2. **For** $i = 2 : N_s$
   Construct CDF: $c_i = c_{i-1} + w_t^i$
   End for
3. $i = 1$
4. Draw a starting point: $u_1 \sim \text{U}[0, 1/N_s]$
5. **For** $j = 1 : N_s$
   $u_j = u_1 + (j-1)/N_s$
   While $u_j > c_i$
   $i = i + 1$
   End while
   $\mathbf{x}_t^j = \mathbf{x}_t^i$
   $w_t^j = 1/N_s$
   End for

B. Particle Filter

Particle filter defines the state space and the measurement models, respectively, as

$$\mathbf{x_t} = \mathbf{f}(\mathbf{x_{t-1}}, \mathbf{v_{t-1}}) \tag{4}$$

$$\mathbf{y_t} = \mathbf{h}(\mathbf{x_t}, \mathbf{n_t}), \tag{5}$$

where $\mathbf{f}$ is the transition function of the state $\mathbf{x}_{t-1}$, $\mathbf{h}$ is the measurement function of $\mathbf{x}_t$, $\mathbf{y}_t$ is received measurement, $\mathbf{n}_t$ and $\mathbf{v}_{t-1}$ are noise. Each iteration is described as the following procedure.

1) Sampling: The sampling stage uses $p(\mathbf{x}_t|\mathbf{x}_{1:t-1}^i)$ from state space model (4) to sample each particles.

2) Weighting: The weighting stage uses $p(\mathbf{x}_t^i|\mathbf{y}_t)$ from the measurement model (5) to obtain pre-normalized weight $\tilde{w}_i$, and then normalizes each weight by the equation

$$w_t^i = \frac{p(\mathbf{y}_t|\mathbf{x}_t^i)}{\sum_{i=1}^{N} p(\mathbf{y}_t|\mathbf{x}_t^i)} \tag{6}$$

3) Resampling: The resampling stage checks whether $N_{eff} < N_T$, where N_T is threshold and N_{eff} is calculated by

$$N_{eff} = \frac{1}{\sum_{i=1}^{N} \left(w_k^i\right)^2}. \tag{7}$$

The particles with the larger weights than N_T are reserved and the particle with smaller weight are discarded. The basic systematic resampling algorithm is described in Table I. The more particles, the more precise posterior pdf can be obtained. A particle filter based on sampling importance resampling (SIR) performs resampling at every iteration.

C. Mixed Norm Distance and Virtual Base-Station Transform

Fig.1 shows the conditions of signal propagation. Fig. 1(a) shows the Euclidean distance $\|(x,y)\|_2 = \sqrt{x^2+y^2}$. Fig. 1(b) shows the Manhattan norm $\|(x,y)\|_1 = |x|+|y|$. In urban area, the signal propagation is usually a mixed path of the Euclidean distance and Manhattan distance, as shown in Fig. 1(c).

A variable $\beta \in [0\ 1]$, called map factor, was proposed to represent the propagation condition [9]. When β=0, it represents the LOS propagation, and when β=1, it presents the Manhattan propagation. The constrained convex optimization problem can be obtained by introducing dummy variable

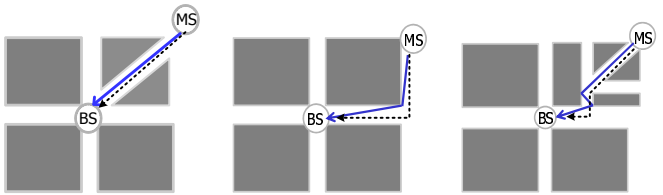

(a) (b) (c)

Fig. 1. (a) Euclidean propagation, (b) Manhattan propagation, and (c) mixed propagation. The solid line represents the actual path and the dotted line represents the approximation path.

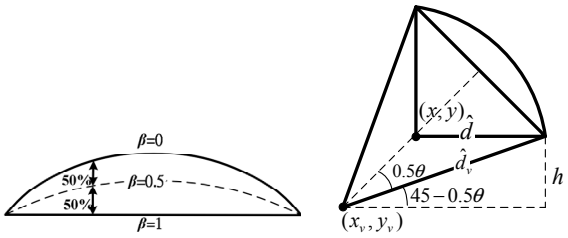

(a) (b)

Fig. 2. (a) Arc curve of $\beta = 0.5$ and (b) the virtual base station transform.

TABLE II. VIRTUAL BS TRANSFORM

$[\hat{d}_v, x_v, y_v] = VBST[\beta, \hat{d}, x_b, y_b, s_1, s_2]$
1. **If** $\beta > 0.95$
   $\beta = 0.95$
   Endif
1. $\theta = (1-\beta) \times 90°$ //central angle
2. $\hat{d}_v = \frac{d}{\sqrt{2}\sin(0.5\theta)}$ //virtual radius
3. $h = r\sin(45 - 0.5\theta)$
4. $(x_v, y_v) = (x_b + s_1 h, y_b + s_2 h)$ //virtual BS

$\hat{d}_v$: virtual radius.
(x_v, y_v): virtual BS. (x_b, y_b): physical BS.

$\mathbf{z} = (z_1, z_2, ..., z_{2n-1}, z_{2n})$ and relaxing the constraints as follows:

$$\min\ f(x,y,\mathbf{z}) = \sum_{i=1}^{n} \{\beta_i \left|z_{2i-1} - \hat{d}_i\right| + (1-\beta_i)\left|z_{2i} - \hat{d}_i\right|\}$$

$$\text{s.t.} \quad \|(x,y)-(x_1,y_1)\|_1 \le z_1, \|(x,y)-(x_1,y_1)\|_2 \le z_2,$$
$$\|(x,y)-(x_2,y_2)\|_1 \le z_3, \|(x,y)-(x_2,y_2)\|_2 \le z_4,$$
$$...$$
$$\|(x,y)-(x_n,y_n)\|_1 \le z_{2n-1}, \|(x,y)-(x_n,y_n)\|_2 \le z_{2n}. \tag{8}$$

where $\hat{d}_i$ is the particle filtered result in the i-th BS. Our previous study [10] extends the map factor β between 0 and 1 for optimization so that the corresponding curve lies between the arc curve and the straight line as shown in Fig. 2(a). The intermediate curve is realized by creating a virtual BS with a larger radius and a farer circle center. The map factor β determines the virtual radius and virtual positions of BSs based on the proposed virtual BS transform (VBST) algorithm in Table II and Fig. 2(b). The s_1 and s_2 in VBST can be easily determined by the relative positions of the BSs.

Then, the constrained convex optimization problem for the

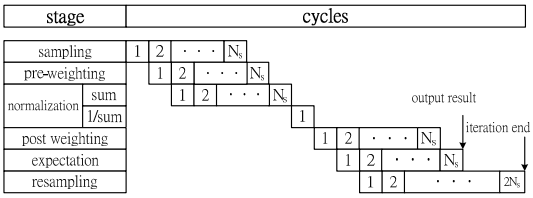

Fig. 3. Timing schedule of a generic particle filter.

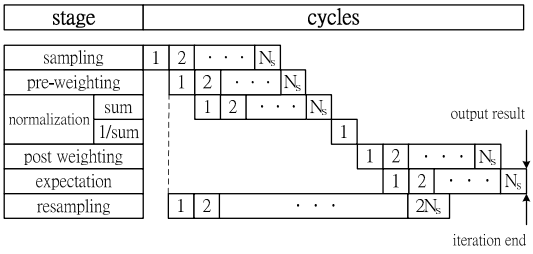

Fig. 4. Timing schedule of the proposed modified resampling particle filter.

mixed propagation becomes

$$\begin{aligned} \min \quad & f(x,y,\mathbf{z}) = \sum_{i=1}^{n} W_{i,d} \left| z_i - \hat{d}_{i,v} \right| \\ \text{s.t.} \quad & \|(x,y) - (x_{j,v}, y_{j,v})\|_2 \le z_j, j = 1...n. \end{aligned} \tag{9}$$

where $W_{i,d}$ is the weight of ith BS; $\hat{d}_{i,v}$ is the virtual radius of ith BS, and $(x_{i,v}, y_{i,v})$ is the virtual coordinate of ith BS. The weight $W_{i,d}$ is

$$W_d = \frac{1}{y} = \frac{1}{ax+b}, \tag{10}$$

where a and b are the coefficients of the fitting curve and x is the estimated distance from the particle filter. The weighting factor reflects a fact that the positioning accuracy is inversely proportional to the relative distance between BS and MS.

III. Particle Filter and Convex Optimization Processor

A. Particle Filter

Fig. 3 shows the timing schedule of a generic particle filter. Note that the end of a iteration and the output result do not occur at the same cycle and there exists additional about N_s cycles because of the resampling process. A generic PF is required to perform resampling process every 10∼20 iterations under a proper value of N_T. This fact implies that if the resampling process can be delayed by a few iterations without much the performance loss. Hence, this study proposes a new resampling method, which delays the resampling process by one iteration as shown in Fig.4.

If the particle filter, in the previous $t-1$-th iteration, identifies that the resampling process is required, the resampling process is performed in the current t-th iteration using the information $w_{t-1}^i, i = 1, 2, ..., N_s$. Then, the particle filter combines the resampling result and current informations of state $x_t^i, i = 1, 2, ..., N_s$. Note that the original resampling process in the generic particle filter uses the information of $w_{t-1}^i, i = 1, 2, ..., N_s$ and $x_{t-1}^i, i = 1, 2, ..., N_s$. For the proposed resmapling method, if some w_{t-1}^is should be

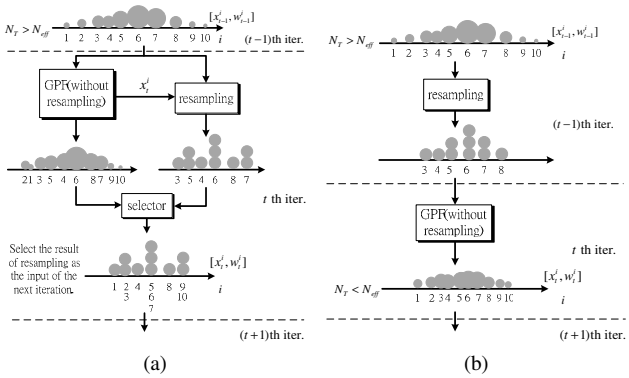

Fig. 5. Comparison of (a) the proposed modified resampling process and (b) the original resampling process for the generic particle filter.

TABLE III. The Proposed Systematic Resampling Algorithm.

$[\{\mathbf{x}_t^j, w_t^j\}_{i=1}^{N_s}] = \text{RESAMPLE}_2[\{\mathbf{x}_t^i, w_t^i\}_{i=1}^{N_s}]$
1. Initial : $c_1 = w_t^1$, $u_1 \sim \text{U}[0, 1/N_s]$, $i = 1$, $j = 1$
2. **For** $n = 1 : 2N_s$
3. **If** $c_i > u_j$
$\mathbf{x}_t^j = \mathbf{x}_t^i$
$w_t^j = 1/N_s$
$u_{j+1} = u_j + 1/N_s$
$j = j + 1$
Else
$c_{i+1} = c_i + w_t^{i+1}$
$i = i + 1$
End if
End for

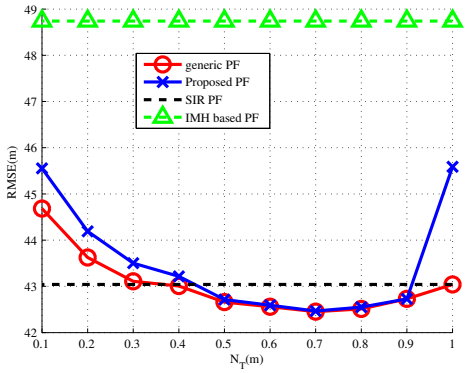

Fig. 6. Performances of the generic, SIR, IMH resampling, and the modified resampling particle filters.

replicated for n particles, the states of the n particles are x_t^i. To avoid obtaining the states of the previous iteration x_{t-1}^i, the proposed particle filter delays a cycle in the resampling processing, as Fig. 4 shows. Fig. 5 shows an example of the resampling process to illustrate the proposed idea. This approach requires additional memories to restore the optional information $w_{k-1}^i, i = 1, 2, ..., N_s$, but it saves N_s cycles.

Fig. 6 shows the the root-mean-squared-error (RMSE) performances versus N_T of the generic particle filter, SIR particle filter, IMH resampling particle filter [11], and the generic particle filter with the modified resampling. Note that SIR particle filter is the special case of $N_T = 1$. The simulation results show that the performance of generic PF and the proposed PF are almost the same in the region of $N_T \in (0.4\ 0.8)$. Table IV compares the RMSE performance, iteration

TABLE IV. COMPARISON OF PARTICLE FILTERS

		SIR PF	GPF	proposed modified resampling PF	IMH resampling based PF
RMSE performance		43.04m	42.45m	42.49m	48.74m
Iteration cycles		$3N_s$ + c	$3N_s$ + c	$2N_s$ + c	N_s + c
MEM	single port	2	2	3	1
	dual port	1	1	2	1

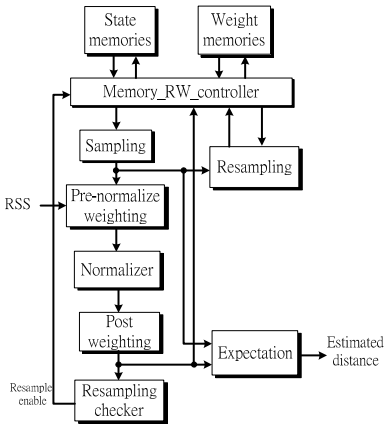

Fig. 7. Block diagram of the proposed particle filter.

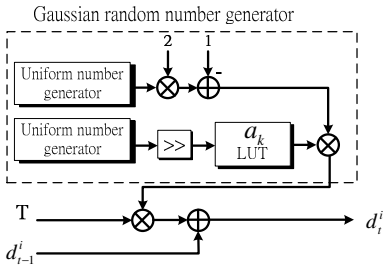

Fig. 8. Sampling function circuit.

cycles, and utilization of memories of different particle filters. The proposed particle filter saves N_S cycles for each iteration and keeps a comparable RMSE performance to the generic and SIR particle filters at sacrifice of memory cost. Fig. 7 shows the block diagram of the particle filter. Each function blocks are described as follows.

1) Sampling: The sampling block calculates

$$d_t^i = d_{t-1}^i + Tv_t^i, \tag{11}$$

where d_t^i and d_{t-1}^i are the relative distance of ith particle of time t and $t-1$, respectively, and v_t^i is a Gaussian random variable realized by Ziggurat algorithm [12]. Fig. 8 shows the sampling function circuit.

2) Weighting: The weighting block generates the weight of each particle by calculating $p(x_t^i|y_t)$ based on the measurement model. The noise is Gaussian distributed so the pre-weighting value is calculated by

$$\tilde{w}_t^i = p(x_t^i|y_t) = w_{t-1}^i \frac{1}{\sqrt{2\pi\sigma^2}} \exp\left(\frac{-\left(P_{ptc(dB)}^i - P_{rx,t(dB)}\right)^2}{2\sigma^2}\right), \tag{12}$$

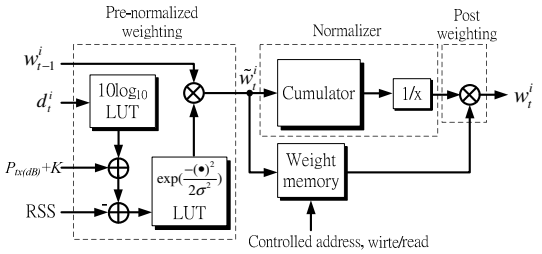

Fig. 9. Architecture of the weighting block.

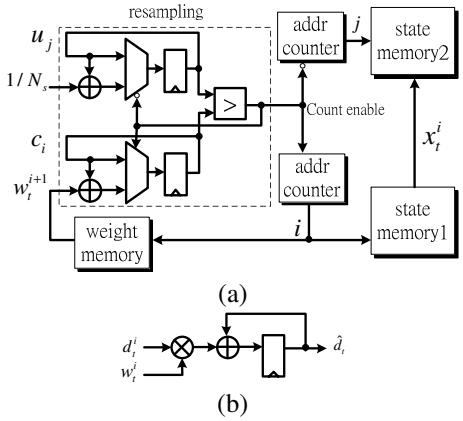

Fig. 10. Architectures of (a) the systematic resampling block and (b) expectation block.

where σ^2 is the variance, $P_{rx,t(dB)}$ is the received RSS measurement at time t, and $P_{ptc(dB)}^i$ is the RSS mapping of the ith particle, which is expressed by

$$P_{ptc(dB)}^i = P_{tx(dB)} + K - 10\log_{10} d_t^i \tag{13}$$

The normalization for the systematic resampling is required to maintain the positioning performance. Due to the normalization, the constant term $1/\sqrt{2\pi\sigma^2}$ can be eliminated and weight calculation (12) can be rewritten as

$$\tilde{w}_t^i = p(x_t^i|y_t) = w_{t-1}^i \exp\left(\frac{-\left(P_{ptc(dB)}^i - P_{rx,t(dB)}\right)^2}{2\sigma^2}\right). \tag{14}$$

Finally, the post-weighting value is given by

$$w_t^i = \frac{\tilde{w}_t^i}{\sum_{i=1}^{N_s} \tilde{w}_t^i}. \tag{15}$$

Fig. 9 shows the weighting block that includes the circuits of the pre-weighting, normalization, and post-weighting.

3) Resampling and Expectation: Fig. 10(a) shows the circuit that realizes the proposed resampling algorithm in Table III. Due to the read/write steps for weight and state memories, the iteration cycles for resampling is $2N_s$. Fig. 10(b) shows the expectation block which is composed of a multiply-and-accumulate operator.

B. Convex optimization processor

Fig. 11 shows the convex optimization processor. A sub-gradient method is used to optimize the particle filter location.

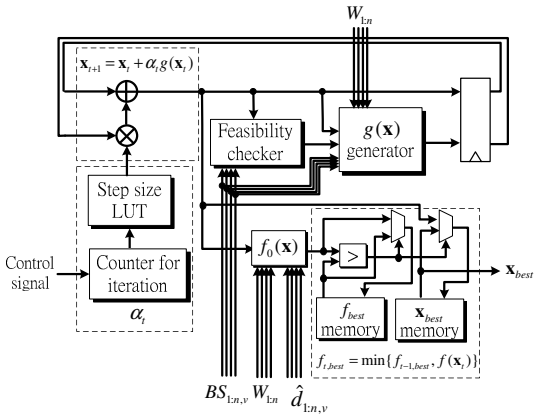

Fig. 11. Architecture of the convex optimization processor based on the constrained sub-gradient method.

It minimizes convex function f by iterating

$$\mathbf{x}_{t+1} = \mathbf{x}_t + \alpha_t g(\mathbf{x}_t). \tag{16}$$

The algorithm searches the point that minimizes f and keeps the best one as expressed by

$$f_{t,best} = \min\{f_{t-1,best}, f(\mathbf{x}_t)\} \tag{17}$$

The search direction $g(\mathbf{x}_t)$ is defined as follows. If $\mathbf{x}_t$ is feasible, $\partial f_0(\mathbf{x}_t)$ is

$$g(\mathbf{x}_t) = \partial f_0(\mathbf{x}_t) = \begin{bmatrix} 0 \\ 0 \\ W_1 \\ W_2 \\ \vdots \\ W_n \end{bmatrix} \tag{18}$$

If $\mathbf{x}_t$ is infeasible,

$$g(\mathbf{x}_t) = \partial f_i(\mathbf{x}_t) = \begin{bmatrix} \frac{2x - 2x_{i,v}}{\|(x,y) - (x_{i,v}, y_{i,v})\|} \\ \frac{2y - 2x_{i,v}}{\|(x,y) - (x_{i,v}, y_{i,v})\|} \\ -\delta(i-1) \\ -\delta(i-2) \\ \vdots \\ -\delta(i-n) \end{bmatrix} \tag{19}$$

for the ith constraint. Fig. 11 shows the architecture of the convex optimization processor. The feasibility checker performs the

$$check_i = \begin{cases} 1, & \text{if } \|(x,y) - BS_{i,v}\|_2 - z_i \le 0 \\ 0, & \text{if } \|(x,y) - BS_{i,v}\|_2 - z_i > 0 \end{cases} \quad i = 1, .., n. \tag{20}$$

as shown in Fig 12(a). Fig. 12(b) shows the $g(\mathbf{x})$ generator. Fig. 12(c)(d) shows the VBST processing blocks and map factor assignment, respectively.

IV. Simulation and Experiment Results

This study uses Xilinx XC4VLX160 FPGA modules, RF Tx/RX modules for WiMax system, and a notebook computer to realize the proposed mobile positioning system, as shown in Fig. 13. Table V lists the FPGA cost of the particle filters and convex optimization processor. Table V also shows the

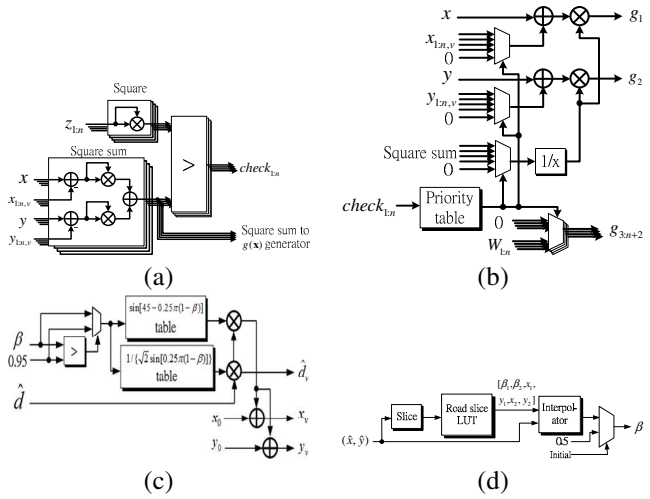

Fig. 12. (a) Feasibility checker. (b) $g(\mathbf{x})$ generator. (c) Virtual base-station transform block. (b) Map factor assignment block.

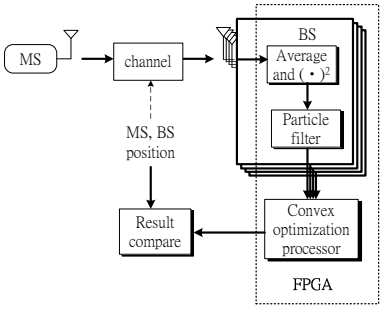

Fig. 13. Positioning system architecture.

TABLE V. FPGA UTILIZATIONS.

Design	The proposed particle filters and convex optimization processor				
Platform	Xilinx Virtex-4 XC4VLS160 FPGA.				
	Slices	Slice Flip Flops	4 input LUTs	Bounded IOBs	DSP48s
Available	67,584	135,168	135,168	768	96
Used	21,464	12,986	15,318	39	46
Utilization rate	31%	9%	11%	5%	47%
Design	Particle filter [13]				
Platform	Xilinx Virtex-5 XC5VSX50T FPGA.				
	Slices	Slice Flip Flops	Slice LUTs	Bounded IOBs	DSP48s
Available	N/A	32,640	32,640	480	288
Used	N/A	13,692	7,379	16	4
Design	Particle filter [14]				
Platform	Xilinx XC2V6000 FPGA.				
	Slices	Slice Flip Flops	Slice LUTs	Bounded IOBs	DSP48s
Available	33,792	67,584	67,584	824	N/A
Used	9,744	7,701	12,089	145	N/A

implementation results of the positioning particle filter in the literature [13], [14]. Although the proposed implementation result has a higher cost, but the proposed system adopte four particle filters for four base-station and a convex optimization processor for the mobile positioning system. After normalization by the particle filter number, the proposed design has lower cost than those of the counterparts. This work used RF TX/RX modules (See Fig. 14(a)) and FPGA modules to construct transmitter and receiver modules. The transmitter module (See Fig. 14(b)) playing the role of mobile station broadcasted OFDM symbols to the wireless environments. The

(a) (b) (c)

Fig. 14. (a) RF module of WiMAX system, (b) the transmitter equipment as mobile station and (b) the receiver equipment as base station.

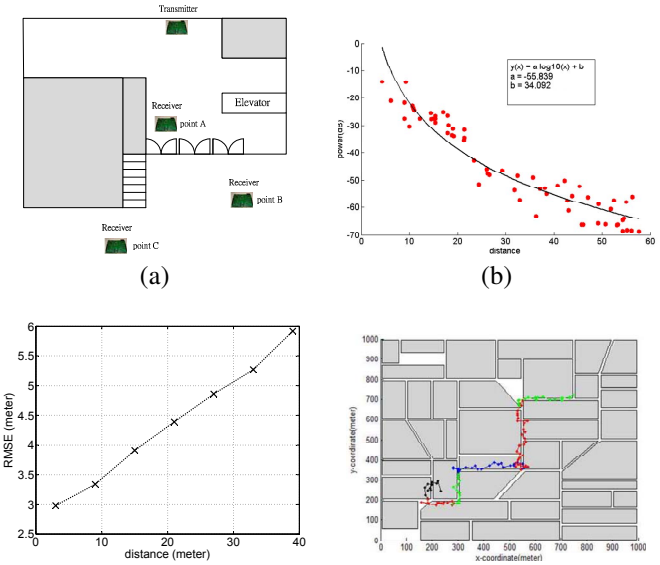

(a) (b) (c) (d)

Fig. 15. (a) Map of 1F TSMC building and the location of Tx/Rx, (b) off-line channel measurements and corresponding fitting curve, (c) measured RMSE analysis results, and (d) simulation map using the practical channel parameters.

receiver module (See Fig. 14(c)) playing the role of base sation collected the received signals as the RSS information in the first floor of the TSMC building in National Tsing Hua University. Fig. 15(a) shows the map of the system experiment environment. The receiver module can be moved to different locations to emulate the operations of multiple base-stations. The experiment used a laser range finder with 15-mm precision to measure the reference location as the benchmark for the positioning system. Before the positioning experiments, the channel path loss parameters were measured to estimate the reference channel gain in the environments. Fig. 15(b) shows the measured results of gain versus distance in the experimental site. The data was used to fit the channel path loss model to obtain the channel parameter as follows:

$$P_{rx(dB)} = P_{tx(dB)} - 10 \times 5.58 \times \log_{10} d + 34.09 \qquad (21)$$

The experiment measured RSS signals at three BS locations and used the particle filters to obtain the filtered distance information. Then, the convex optimization processor was used to optimize the location information based on three distance results of three BS locations. Fig. 15(c) shows the RMSE analysis results of the on-site measurement. The proposed positioning system achieves 3∼6-meter error in the mixed NLOS-LOS environment of Fig. 15(a). In additional, we used the parameters in (21) to simulate the channel and analyzed the RMSE of positioning the MS route in the map of Fig. 15(d), where four BS lie at corners. The distance outputs of the particle filters achieved 36.9-meter RMSE precision, while the positioning results achieved 29.2-meter RMSE precision. The precision improvement is mainly contributed by the VBST and convex optimization processings.

V. Conclusion

This paper presents the realization of a network-based positioning system. The particle filter and convex optimization processor were designed and implemented in the FPGA chip. The system integrates RF TX/RX and the FPGA modules to realize the positioning system. The measurement and simulation results show that the proposed algorithm reduces 20% positioning RMSE error by dealing with the NLOS problem.

References

[1] I. Paton, E. Crompton, J. Gardiner, and J. Noras, "Terminal self-location in mobile radio systems," in *Mobile Radio and Personal Communications, 1991., Sixth International Conference on*, dec 1991, pp. 203 –207.

[2] H. Hashemi, "Pulse ranging radiolocation technique and its application to channel assignment in digital cellular radio," in *Vehicular Technology Conference, 1991. Gateway to the Future Technology in Motion., 41st IEEE*, may 1991, pp. 675 –680.

[3] A. Giordano, M. Chan, and H. Habal, "A novel location-based service and architecture," in *Personal, Indoor and Mobile Radio Communications, 1995. PIMRC'95. 'Wireless: Merging onto the Information Superhighway'., Sixth IEEE International Symposium on*, vol. 2, sep 1995, pp. 853 –857 vol.2.

[4] H. Koshima and J. Hoshen, "Personal locator services emerge," *Spectrum, IEEE*, vol. 37, no. 2, pp. 41 –48, feb 2000.

[5] T. Kerr, "A critical perspective on some aspects of gps development and use," in *Digital Avionics Systems Conference, 1997. 16th DASC., AIAA/IEEE*, vol. 2, oct 1997, pp. 9.4 –9–9.4–20 vol.2.

[6] M. Arulampalam, S. Maskell, N. Gordon, and T. Clapp, "A tutorial on particle filters for online nonlinear/non-gaussian bayesian tracking," *Signal Processing, IEEE Transactions on*, vol. 50, no. 2, pp. 174 –188, feb 2002.

[7] B. Ristic, S. Arulampalm, and N. Gordon, *Beyond the Kalman filter : particle filters for tracking applications*. Artech House, Boston, Ma. ; London :, 2004.

[8] S. Al-Jazzar, J. Caffery, and H.-R. You, "Scattering-model-based methods for toa location in nlos environments," *Vehicular Technology, IEEE Transactions on*, vol. 56, no. 2, pp. 583 –593, march 2007.

[9] W.-Y. Chiu and B.-S. Chen, "Mobile location estimation in urban areas using mixed manhattan/euclidean norm and convex optimization," *Wireless Communications, IEEE Transactions on*, vol. 8, no. 1, pp. 414 –423, jan. 2009.

[10] L.-H. Huang, K.-T. Shr, and Y.-H. Huang, "Mobile positioning system based on virtual base station transform and convex optimization," in *IEEE Workshop on Signal Processing Systems (SiPS 2012)*, vol. 4, oct. 2012.

[11] A. Sankaranarayanan, R. Chellappa, and A. Srivastava, "Algorithmic and architectural design methodology for particle filters in hardware," in *Computer Design: VLSI in Computers and Processors, 2005. ICCD 2005. Proceedings. 2005 IEEE International Conference on*, oct. 2005, pp. 275 – 280.

[12] G. Marsaglia and W. W. Tsang, "The ziggurat method for generating random variables," *Journal of Statistical Software*, vol. 5, no. 8, pp. 1–7, 10 2000. [Online]. Available: http://www.jstatsoft.org/v05/i08

[13] B. Ye and Y. Zhang, "Improved fpga implementation of particle filter for radar tracking applications," in *Synthetic Aperture Radar, 2009. APSAR 2009. 2nd Asian-Pacific Conference on*, oct. 2009, pp. 943 –946.

[14] J. U. Cho, S. H. Jin, X. D. Pham, and J. W. Jeon, "Object tracking circuit using particle filter with multiple features," in *SICE-ICASE, 2006. International Joint Conference*, oct. 2006, pp. 1431 –1436.